PERGAMON

International Journal of Solids and Structures 39 (2002) 1097–1117

INTERNATIONAL JOURNAL OF SOLIDS and STRUCTURES

www.elsevier.com/locate/ijsolstr

Electroelastic analysis of an anti-plane shear crack in a piezoelectric ceramic strip

Xian-Fang Li

College of Mathematics and Physics, Hunan Normal University, Changsha, Hunan 410081, China

Received 6 June 2001

Abstract

The electroelastic analysis of a piezoelectric strip with an anti-plane shear crack whose surfaces are parallel to the strip boundaries is made. Four cases of combined electromechanical loadings applied at the strip boundaries are considered. For the case of a crack lying at the center of a strip, the electroelastic field, field intensity factors, and energy release rate can be determined in explicit form via solving a resulting singular integral equation. For other cases, they can be given in terms of an auxiliary function, which is obtained as a power series of δ via solving a resulting Fredholm integral equation using the iterative method, 2δ being the ratio of the crack length over the strip width. Some numerical results are presented graphically to show the influence of crack length and crack position on the normalized energy release rate. © 2002 Elsevier Science Ltd. All rights reserved.

Keywords: Piezoelectric strip; Anti-plane shear crack; Field intensity factors; Energy release rate

1. Introduction

Due to the intrinsic coupling characteristics between electric and elastic behaviors, piezoelectric materials have been used widely in technology such as transducers, actuators, sensors, etc. Great progress on the study of electroelastic field disturbed by cracks in a piezoelectric material has been made in recent years. Considerable researches in this area are mainly focused on determining the electroelastic field under various different boundary conditions within the framework of the theory of reigning linear piezoelectricity. Many theoretical solutions of crack problems have been derived under the assumption of several different electric boundary conditions at the crack surfaces (see, for example, Pak, 1990, 1992; Sosa, 1991, 1992; Suo et al., 1992; Wang, 1992; Dunn, 1994; Park and Sun, 1995a; Dascalu and Maugin, 1995; Sosa and Khutoryansky, 1996; Zhang and Tong, 1996; Zhang et al., 1998; Zhong and Meguid, 1997; Wang and Han, 1999; Chen and Shioya, 1999; Yang, 2001).

The above-mentioned solutions are mainly related to internal cracks embedded in a piezoelectric material. In general, in engineering applications the structure of piezoelectric devices is frequently met as a

E-mail address: lixf@mail.hunnu.edu.cn (X.-F. Li).

PII: S0020-7683(01)00251-7

layered medium. Therefore, to secure the structural integrity of these piezoelectric devices, the problem posed with a layered piezoelectric medium containing cracks is of much interest. As a result, determining the electric and elastic behaviors disturbed by a crack in a layered piezoelectric material, in particular in the close vicinity of the through crack tip, is prerequisite. For a piezoelectric layer or strip with a crack, Shindo and coworkers made systematic investigation on the electroelastic analysis. The problems involving a central permeable crack parallel to and perpendicular to the strip boundaries have been studied by Shindo et al. (1990, 2000), respectively. Furthermore, they also investigated the corresponding electroelastic problems for a central anti-plane shear crack (Shindo et al., 1996, 1997). More recently, the electroelastic analysis of a rectangular sheet containing a central permeable crack subjected to anti-plane electromechanical loadings has been made by Kwon and Lee (2000), and the problem of a piezoelectric strip with a crack under in-plane electromechanical loadings has been analyzed by Wang et al. (2000), who compared the results based on the permeability assumption with those based on the impermeability assumption. The interface crack problem of a layered bimaterial composed of a piezoelectric material and a purely elastic orthotropic medium has been considered by Narita and Shindo (1999).

This paper is concerned with the problem of an internal anti-plane shear crack embedded a piezoelectric strip subjected to four cases of combined electromechanical loadings. The crack surfaces are assumed to be parallel to the boundary surfaces of the strip and the crack is not necessarily located at the center of a strip. Using the integral transform technique, the associated mixed boundary value problem is reduced to dual integral equations, which are further transformed into a Fredholm integral equation by introducing an auxiliary function. The iterative method for seeking an approximate solution is employed to solve the resulting Fredholm integral equation in this paper, which is in contrast to those adopted by Shindo et al. (1990, 1997), Shin et al. (2000) and Wang et al. (2000), who determined numerically the electroelastic field via solving numerically a Fredholm integral equation. Then electroelastic field, field intensity factors and energy release rate as well, are given explicitly in terms of the auxiliary function. In particular, for a special case of a crack lying at the center of a strip, a closed-form solution is obtained via solving analytically a singular integral equation. Finally, some numerical results are presented graphically to show the effects of the crack position and the crack length on the normalized energy release rate.

2. Statement of the problem and basic theory

Consider a piezoelectric layer which has infinite extent in the xz-plane and finite size of thickness $2h$ ($2h = h_1 + h_2$) along the y-axis direction. A through crack of length $2a$ is located at the plane $y = 0$, and the crack boundaries are parallel to the z-axis, as shown in Fig. 1. Here Cartesian coordinates x, y, z are the principal axes of the material symmetry while the z-axis is oriented in the poling direction of the piezoelectric strip. Four possible cases of combined electromechanical loadings will be considered. They are

Case 1: uniform longitudinal shear stresses and constant electric displacements at the top and bottom surfaces of the layer, i.e.

$$\tau_{zy}(x, h_1) = \tau_{zy}(x, -h_2) = \tau_0, \quad D_y(x, h_1) = D_y(x, -h_2) = D_0, \qquad -\infty < x < \infty; \tag{1}$$

Case 2: uniform longitudinal shear stresses at the top and bottom boundaries and constant voltage (or electric potential difference) between the top and the bottom surface of the layer, i.e.

$$\tau_{zy}(x, h_1) = \tau_{zy}(x, -h_2) = \tau_0, \quad \phi(x, h_1) - \phi(x, -h_2) = -2V_0, \qquad -\infty < x < \infty; \tag{2}$$

Case 3: constant relative sliding displacement along the z-axis between the top and the bottom surface and constant electric displacements at the top and bottom surfaces of the layer, i.e.

$$w(x, h_1) - w(x, -h_2) = 2w_0, \quad D_y(x, h_1) = D_y(x, -h_2) = D_0, \qquad -\infty < x < \infty; \tag{3}$$

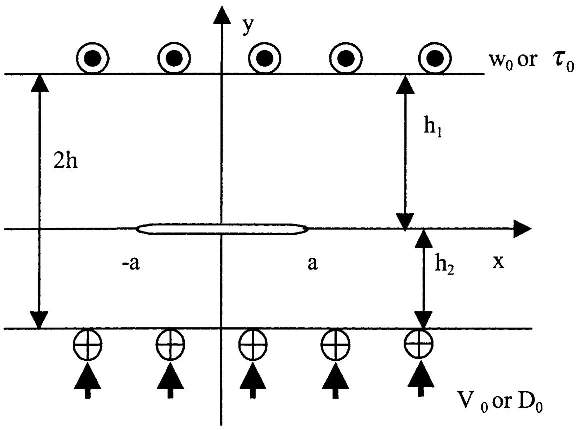

Fig. 1. Schematic of a through anti-plane shear crack in a piezoelectric strip.

Case 4: constant relative sliding displacement along the z-axis and the voltage (or electric potential difference) between the top and the bottom surface of the layer, i.e.

$$w(x, h_1) - w(x, -h_2) = 2w_0, \quad \phi(x, h_1) - \phi(x, -h_2) = -2V_0, \qquad -\infty < x < \infty. \tag{4}$$

Since the piezoelectric strip in question are in a state of longitudinal shear deformation, or anti-plane deformation with respect to the xy-plane, in this case one can take a plane normal to the z-axis as the plane of concern, and so the following analysis is restricted to the strip in this plane. Under such circumstances, there are only nonvanishing the out-of-plane displacement $w(x, y)$ and the in-plane electric potential $\phi(x, y)$, which satisfy the basic governing field equations for anti-plane piezoelectricity, in the absence of body force and free charge (Parton and Kudryavsev, 1988),

$$\begin{aligned} c_{44}\nabla^2 w + e_{15}\nabla^2\phi = 0, \\ e_{15}\nabla^2 w - \varepsilon_{11}\nabla^2\phi = 0, \end{aligned} \tag{5}$$

where c_{44} is the elastic stiffness measured in a constant electric field, ε_{11} is the dielectric permittivity measured at a uniform strain, e_{15} is the piezoelectric constant of the piezoelectric strip, and $\nabla^2 = \partial^2/\partial x^2 + \partial^2/\partial y^2$ represents the two-dimensional Laplacian operator.

Once functions w and ϕ are determined from the given conditions, then the components of anti-plane shear stress and in-plane electric displacement in a piezoelectric strip are obtainable in terms of the following constitutive equations:

$$\tau_{zx} = c_{44}\gamma_{zx} - e_{15}E_x, \quad \tau_{zy} = c_{44}\gamma_{zy} - e_{15}E_y, \tag{6}$$

$$D_x = e_{15}\gamma_{zx} + \varepsilon_{11}E_x, \quad D_y = e_{15}\gamma_{zy} + \varepsilon_{11}E_y, \tag{7}$$

where anti-plane strain and electric field in a piezoelectric strip are given as follows:

$$\gamma_{zx} = \frac{\partial w}{\partial x}, \quad \gamma_{zy} = \frac{\partial w}{\partial y}, \tag{8}$$

$$E_x = -\frac{\partial\phi}{\partial x}, \quad E_y = -\frac{\partial\phi}{\partial y}. \tag{9}$$

To seek the electroelastic field in a piezoelectric strip, the elastic and electric boundary conditions at the crack surfaces must be furnished. It is evident that for mechanical field, the crack surfaces are free of stress, i.e.

$$\tau_{zy}(x,0^+) = \tau_{zy}(x,0^-) = 0, \quad |x| < a. \tag{10}$$

For electric field, there exist some different opinions on the electric boundary conditions at the crack surfaces. One opinion assumes that the crack surfaces is impermeable to electric field (Pak, 1990, 1992; Sosa, 1991, 1992; Suo et al., 1992; Wang, 1992; Zhong and Meguid, 1997; Chen and Shioya, 1999; etc.), and another opinion assumes that the crack surfaces is permeable to electric field (Parton, 1976; Meguid and Wang, 1998; Wang and Han, 1999; Wang, 2001; Yang, 2001; etc.). According to the analyses in Dunn (1994), Sosa and Khutoryansky (1996) and Zhang and Tong (1996), the impermeable assumption may give rise to a significant error in analyzing electroelastic field of a crack. The choice of between these two types of electric boundary conditions is analyzed deeply from the viewpoint of energy balance in the context of the Griffith fracture theory by Dascalu (1997). On the other hand, for anti-plane shear problems, the upper and lower surfaces of a crack contact each other, and they continue to contact under the action of anti-plane mechanical loadings and in-plane electric loadings. Therefore, the permeable electric boundary conditions will be assumed in the present paper. That is, both the electric potential and the normal electric displacement are assumed to be continuous across the crack surfaces, which can be stated below

$$\phi(x,0^+) = \phi(x,0^-), \quad D_y(x,0^+) = D_y(x,0^-), \qquad |x| < a. \tag{11}$$

In effect, since $E_x = -\partial\phi/\partial x$, it is easily found that the above electric boundary conditions are equivalent to those adopted by Shindo et al. (1990, 1996, 1997, 2000) in a series of papers involving the electroelastic analyses of cracks in a piezoelectric material, i.e.

$$E_x(x,0^+) = E_x(x,0^-) = E_x^c(x,0), \quad D_y(x,0^+) = D_y(x,0^-) = D_y^c(x,0), \qquad |x| < a, \tag{12}$$

where the superscript c represents the electric quantities in the void inside the crack.

Meanwhile, the elastic and electric field should fulfil the following continuity conditions along the line $y = 0$:

$$w(x,0^+) = w(x,0^-), \quad \phi(x,0^+) = \phi(x,0^-), \qquad |x| \geqslant a, \tag{13}$$

$$\tau_{zy}(x,0^+) = \tau_{zy}(x,0^-), \quad D_y(x,0^+) = D_y(x,0^-), \qquad -\infty < x < \infty. \tag{14}$$

Due to the symmetry of the problem under consideration, it is sufficient to analyze the right-half portion, i.e. $x > 0$. Therefore in the following the electroelastic field in the region $x > 0$ is concerned and that in the remaining section can be directly given by symmetry.

In order to obtain the desired electroelastic field, it is convenient to separate the problem considered into two subproblems, one corresponding to the piezoelectric strip with no crack and the other corresponding to the piezoelectric strip with a crack for which the anti-plane shear stress applied at the crack surfaces are prescribed as the negative of those produced by the former, and the strip boundaries are also governed by appropriate conditions (see below). For the former, a uniform field is produced, in which the components of anti-plane shear stresses and electric displacements can be expressed as:

$$\tau_{zy}(x,y) = \tau_0, \quad D_y(x,y) = D_0 \quad \text{for case 1}, \tag{15}$$

$$\tau_{zy}(x,y) = \tau_0, \quad D_y(x,y) = \frac{e_{15}}{c_{44}}\tau_0 + \left(\varepsilon_{11} + \frac{e_{15}^2}{c_{44}}\right)\frac{V_0}{h} \quad \text{for case 2}, \tag{16}$$

$$\tau_{zy}(x,y) = \left(c_{44} + \frac{e_{15}^2}{\varepsilon_{11}}\right)\frac{w_0}{h} - \frac{e_{15}}{\varepsilon_{11}}D_0, \quad D_y(x,y) = D_0 \quad \text{for case 3,} \tag{17}$$

$$\tau_{zy}(x,y) = \frac{c_{44}w_0 - e_{15}V_0}{h}, \quad D_y(x,y) = \frac{e_{15}w_0 + \varepsilon_{11}V_0}{h} \quad \text{for case 4.} \tag{18}$$

For the latter, a singular field arises, which can be solved from the following electroelastic boundary conditions:

at the line $y = 0$,

$$\tau_{zy}(x,0^+) = \tau_{zy}(x,0^-) = -\tau^{(l)}, \quad \phi(x,0^+) = \phi(x,0^-), \quad D_y(x,0^+) = D_y(x,0^-), \qquad |x| < a, \tag{19}$$

$$\tau_{zy}(x,0^+) = \tau_{zy}(x,0^-), \quad w(x,0^+) = w(x,0^-), \qquad |x| \geqslant a, \tag{20}$$

$$\phi(x,0^+) = \phi(x,0^-), \quad D_y(x,0^+) = D_y(x,0^-), \qquad |x| \geqslant a \tag{21}$$

and at the strip boundaries,

$$\text{case 1:} \quad \tau_{zy}(x,h_1) = \tau_{zy}(x,-h_2) = 0, \quad D_y(x,h_1) = D_y(x,-h_2) = 0, \qquad -\infty < x < \infty; \tag{22}$$

$$\text{case 2:} \quad \tau_{zy}(x,h_1) = \tau_{zy}(x,-h_2) = 0, \quad \phi(x,h_1) = \phi(x,-h_2) = 0, \qquad -\infty < x < \infty; \tag{23}$$

$$\text{case 3:} \quad w(x,h_1) = w(x,-h_2) = 0, \quad D_y(x,h_1) = D_y(x,-h_2) = 0, \qquad -\infty < x < \infty; \tag{24}$$

$$\text{case 4:} \quad w(x,h_1) = w(x,-h_2) = 0, \quad \phi(x,h_1) = \phi(x,-h_2) = 0, \qquad -\infty < x < \infty, \tag{25}$$

where $\tau^{(l)}$ represents the value of $\tau_{zy}(x,0)$ at the corresponding case, $l = 1, 2, 3, 4$, given by Eqs. (15)–(18), respectively.

From the viewpoint of fracture mechanics, of importance is the singular field disturbed by a crack. Consequently, in what follows we restrict our attention to solving the singular field. To achieve this, an integral transform technique is employed to reduce the latter posed by Eqs. (19)–(21) and one of Eqs. (22)–(25) into dual integral equations. By use of the Fourier transform, it is easily shown that appropriate solution of Eq. (5) can be expressed as the following integrals

$$w_j(x,y) = \int_0^\infty [A_j(\xi)\cosh(y\xi) + B_j(\xi)\sinh(y\xi)]\cos(x\xi)\,\mathrm{d}\xi, \quad x \geqslant 0, \tag{26}$$

$$\phi_j(x,y) = \int_0^\infty [C_j(\xi)\cosh(y\xi) + D_j(\xi)\sinh(y\xi)]\cos(x\xi)\,\mathrm{d}\xi, \quad x \geqslant 0, \tag{27}$$

where $A_j(\xi), \ldots, D_j(\xi)$ are unknown to be determined from given conditions, and $j = 1, 2$ correspond to the regions $y \geqslant 0$ and $y \leqslant 0$, respectively.

With the aid of constitutive equations, from Eqs. (26) and (27) it is not difficult to obtain the expressions for the components of the stress, strain, electric displacement and electric field in terms of $A, \ldots, D$. For example, we have

$$\tau_{zyj} = \int_0^\infty \xi[(c_{44}A_j + e_{15}C_j)\sinh(y\xi) + (c_{44}B_j + e_{15}D_j)\cosh(y\xi)]\cos(x\xi)\,\mathrm{d}\xi, \tag{28}$$

$$D_{yj} = \int_0^\infty \xi[(e_{15}A_j - \varepsilon_{11}C_j)\sinh(y\xi) + (e_{15}B_j - \varepsilon_{11}D_j)\cosh(y\xi)]\cos(x\xi)\,\mathrm{d}\xi. \tag{29}$$

3. Solution procedure

In this section, our objective is to determine the singular electroelastic field induced by an anti-plane shear crack and to give expressions for the relevant physical quantities including field intensity factors and energy release rate. Here, without loss of generality, suppose that $h_1 \geqslant h_2$, which means that a crack may not be located at the center of the strip, h_1 and h_2 being the distance between the crack surface and the top boundary of the strip, and the crack surface and the bottom boundary of the strip, respectively.

First, from the continuity conditions along the line $y = 0$, i.e.

$$\tau_{zy1}(x,0) = \tau_{zy2}(x,0), \quad \phi_1(x,0) = \phi_2(x,0), \quad D_{y1}(x,0) = D_{y2}(x,0), \tag{30}$$

we find

$$B_1 = B_2, \quad C_1 = C_2, \quad D_1 = D_2. \tag{31}$$

Then one can easily show that the sliding displacement across the line $y = 0$ and the stress component at the line $y = 0$ are expressed by the following integrals, respectively,

$$w_1(x,0) - w_2(x,0) = \int_0^\infty (A_1 - A_2)\cos(x\xi)\,\mathrm{d}\xi, \quad x \geqslant 0, \tag{32}$$

$$\tau_{zyj}(x,0) = \int_0^\infty \xi(c_{44}B_1 + e_{15}D_1)\cos(x\xi)\,\mathrm{d}\xi, \quad x \geqslant 0. \tag{33}$$

Furthermore, for case 1, the boundary surfaces $y = h_1$ and $y = -h_2$ of the strip are free of stress and of electric displacement, i.e. Eq. (22). Using Eqs. (28) and (29), from Eq. (22) we get

$$A_1\sinh(h_1\xi) + B_1\cosh(h_1\xi) = 0, \quad C_1\sinh(h_1\xi) + D_1\cosh(h_1\xi) = 0, \tag{34}$$

$$A_2\sinh(h_2\xi) - B_2\cosh(h_2\xi) = 0, \quad C_2\sinh(h_2\xi) - D_2\cosh(h_2\xi) = 0. \tag{35}$$

Putting Eq. (31) into Eqs. (34) and (35) yields

$$A_2 = -A_1\tan(h_1\xi)\coth(h_2\xi), \quad C_2 = C_1 = D_1 = D_2 = 0. \tag{36}$$

The remaining unknown function A_1 can be determined from the remaining mechanical boundary conditions, i.e. the first in Eq. (19) and the second in Eq. (20), which, in connection with Eqs. (32) and (33), then become a pair of simultaneous dual integral equations for A_1

$$\int_0^\infty [1 + \tan(h_1\xi)\coth(h_2\xi)]A_1(\xi)\cos(x\xi)\,\mathrm{d}\xi = 0, \quad |x| \geqslant a, \tag{37}$$

$$-c_{44}\int_0^\infty \xi A_1(\xi)\tanh(h_1\xi)\cos(x\xi)\,\mathrm{d}\xi = -\tau^{(1)}, \quad |x| < a. \tag{38}$$

In general, it is difficult to obtain a closed-form solution of the resulting dual integral equations except for a particular case where a crack is situated at the center of a strip, i.e. $h_1 = h_2$, for which we shall give a closed-form solution in the next section. Here we first study the case of $h_1 \geqslant h_2$, and the case of $h_1 \leqslant h_2$ is completely similar to the former. For this case, by using the techniques, outlined in Sneddon (1972) and others, the dual integral equations can be transformed into a Fredholm integral equation of the second kind. To achieve this, we choose $A_1(\xi)$ given by

$$A_1(\xi) = \frac{2}{1 + \tan(h_1\xi)\coth(h_2\xi)}\int_0^a \psi(u)J_0(u\xi)\,\mathrm{d}u, \tag{39}$$

where $J_0(\ )$ denotes the Bessel function of the first kind of order zero and $\psi(u)$ is an auxiliary function.

Recalling the results (Gradshteyn and Ryzhik, 1980)

$$\int_0^\infty J_0(u\xi)\cos(x\xi)\,\mathrm{d}\xi = 0, \quad x > u \tag{40}$$

and

$$J_0(x\xi) = \frac{2}{\pi}\int_0^x \frac{\cos(t\xi)}{\sqrt{x^2 - t^2}}\,\mathrm{d}t, \tag{41}$$

it is easily shown that Eq. (37) will be automatically satisfied. Eq. (38) then becomes the following Fredholm integral equation of the second kind

$$\psi(x) + \int_0^a K^{(1)}(x,u)\psi(u)\,\mathrm{d}u = \frac{x\tau^{(1)}}{c_{44}}, \quad 0 \leqslant x < a \tag{42}$$

with

$$K^{(1)}(x,u) = x\int_0^\infty \left[\frac{2}{\coth(h_1\xi) + \coth(h_2\xi)} - 1\right]\xi J_0(u\xi)J_0(x\xi)\,\mathrm{d}\xi. \tag{43}$$

For case 2, the boundary surfaces $y = h_1$ and $y = -h_2$ of the strip are stress-free and grounded, i.e. Eq. (23). A completely similar procedure leads to a pair of dual integral equations for A_1 for case 2, which are the same as the ones for case 1 and hence the Fredholm integral equation for the case 2 is also governed by Eq. (42). It is noted that the only discrepancy between electroelastic fields for the cases 1 and 2 lies in their individual uniform electroelastic fields.

For case 3, the boundary surfaces $y = h_1$ and $y = -h_2$ of the strip are fixed and free of electric displacement, i.e. Eq. (24). In this case from Eq. (24) we have

$$A_1\cosh(h_1\xi) + B_1\sinh(h_1\xi) = 0, \tag{44}$$

$$A_2\cosh(h_2\xi) - B_2\sinh(h_2\xi) = 0, \tag{45}$$

$$(e_{15}A_1 - \varepsilon_{11}C_1)\sinh(h_1\xi) + (e_{15}B_1 - \varepsilon_{11}D_1)\cosh(h_1\xi) = 0, \tag{46}$$

$$-(e_{15}A_2 - \varepsilon_{11}C_2)\sinh(h_2\xi) + (e_{15}B_2 - \varepsilon_{11}D_2)\cosh(h_2\xi) = 0, \tag{47}$$

which, together with Eq. (31), can be solved in terms of A_1

$$A_2 = -A_1\coth(h_1\xi)\tan(h_2\xi), \tag{48}$$

$$B_1 = B_2 = -A_1\coth(h_1\xi), \tag{49}$$

$$C_1 = C_2 = \frac{e_{15}}{\varepsilon_{11}}A_1\coth(h_1\xi)[\tan(h_1\xi) - \tan(h_2\xi)], \tag{50}$$

$$D_1 = D_2 = \frac{e_{15}}{\varepsilon_{11}}A_1\coth(h_1\xi)[\tan(h_1\xi)\tan(h_2\xi) - 1]. \tag{51}$$

Upon substitution of these into Eqs. (32) and (33) yields a pair of dual integral equations for A_1,

$$\int_0^\infty [1 + \coth(h_1\xi)\tan(h_2\xi)]A_1(\xi)\cos(x\xi)\,\mathrm{d}\xi = 0, \quad |x| \geqslant a, \tag{52}$$

$$\int_0^\infty \xi\left[1 + \frac{e_{15}^2}{c_{44}\varepsilon_{11}}(1 - \tanh(h_1\xi)\tanh(h_2\xi))\right]\coth(h_1\xi)A_1(\xi)\cos(x\xi)\,\mathrm{d}\xi = \frac{\tau^{(3)}}{c_{44}}, \quad |x| < a. \tag{53}$$

Similarly, if we take

$$A_1(\xi) = \frac{2}{1 + \coth(h_1\xi)\tan(h_2\xi)} \int_0^a \psi(u) J_0(u\xi)\,\mathrm{d}u, \tag{54}$$

Eq. (52) is automatically satisfied and Eq. (53) is then transformed to

$$\psi(x) + \int_0^a K^{(3)}(x,u)\psi(u)\,\mathrm{d}u = \frac{x\tau^{(3)}}{c_{44}}, \quad 0 \leqslant x < a \tag{55}$$

with

$$K^{(3)}(x,u) = x\int_0^\infty \left[\frac{2c_{44}\varepsilon_{11} + e_{15}^2(1 - \tanh(h_1\xi)\tanh(h_2\xi))}{c_{44}\varepsilon_{11}(\tanh(h_1\xi) + \tanh(h_2\xi))} - 1\right]\xi J_0(u\xi)J_0(x\xi)\,\mathrm{d}\xi. \tag{56}$$

For case 4, the boundary surfaces $y = h_1$ and $y = -h_2$ of the strip are fixed and grounded, i.e. Eq. (25). Using Eqs. (26) and (27) we get

$$A_1\cosh(h_1\xi) + B_1\sinh(h_1\xi) = 0, \quad C_1\cosh(h_1\xi) + D_1\sinh(h_1\xi) = 0; \tag{57}$$

$$A_2\cosh(h_2\xi) - B_2\sinh(h_2\xi) = 0, \quad C_2\cosh(h_2\xi) - D_2\sinh(h_2\xi) = 0. \tag{58}$$

Thus, we deduce to

$$A_2 = -A_1\coth(h_1\xi)\tan(h_2\xi), \quad C_2 = -C_1\coth(h_1\xi)\tan(h_2\xi) \tag{59}$$

from which in connection with Eq. (31), it follows that

$$C_2 = C_1 = D_1 = D_2 = 0. \tag{60}$$

Consequently, one can easily show in this case that the remaining mechanical boundary conditions, i.e. the first in Eq. (19) and the second in Eq. (20), in connection with Eqs. (32) and (33), result into a pair of simultaneous dual integral equations for A_1 as follows

$$\int_0^\infty [1 + \coth(h_1\xi)\tan(h_2\xi)]A_1(\xi)\cos(x\xi)\,\mathrm{d}\xi = 0, \quad |x| \geqslant a, \tag{61}$$

$$-c_{44}\int_0^\infty \xi A_1(\xi)\coth(h_1\xi)\cos(x\xi)\,\mathrm{d}\xi = -\tau^{(4)}, \quad |x| < a. \tag{62}$$

Likewise, if we take $A_1(\xi)$ in the form of Eq. (54), Eq. (61) is automatically satisfied and Eq. (62) is transformed to

$$\psi(x) + \int_0^a K^{(4)}(x,u)\psi(u)\,\mathrm{d}u = \frac{x\tau^{(4)}}{c_{44}}, \quad 0 \leqslant x < a \tag{63}$$

with

$$K^{(4)}(x,u) = x\int_0^\infty \left[\frac{2}{\tanh(h_1\xi) + \tanh(h_2\xi)} - 1\right]\xi J_0(u\xi)J_0(x\xi)\,\mathrm{d}\xi. \tag{64}$$

For the purpose of computation, introducing dimensionless variables

$$\bar{x} = \frac{x}{a}, \quad \bar{u} = \frac{u}{a}, \quad \bar{\psi}(\bar{x}) = \frac{\psi(a\bar{x})}{a}, \tag{65}$$

the Fredholm integral equations obtained above for all the four cases can be rewritten in dimensionless form

$$\bar{\psi}(\bar{x}) + \int_0^1 \bar{K}^{(l)}(\bar{x},\bar{u})\bar{\psi}(\bar{u})\,\mathrm{d}\bar{u} = \frac{\bar{x}\tau^{(l)}}{c_{44}}, \quad 0 \leqslant \bar{x} < 1, \;\; l = 1,2,3,4, \tag{66}$$

where

$$\bar{K}^{(l)}(\bar{x},\bar{u}) = \delta^2 \bar{x} \int_0^\infty \eta k^{(l)}(\eta) J_0(\bar{u}\eta\delta) J_0(\bar{x}\eta\delta)\,\mathrm{d}\eta \tag{67}$$

with

$$k^{(1)}(\eta) = k^{(2)}(\eta) = \frac{1}{\sinh(\eta)}\left[\mathrm{e}^{-\eta} - \cosh\left(\frac{\alpha-1}{\alpha+1}\eta\right)\right], \tag{68}$$

$$k^{(3)}(\eta) = \frac{1}{\sinh(\eta)}\left[\left(1 + \frac{2e_{15}^2}{c_{44}\varepsilon_{11}}\right)\cosh\left(\frac{\alpha-1}{\alpha+1}\eta\right) + \mathrm{e}^{-\eta}\right], \tag{69}$$

$$k^{(4)}(\eta) = \frac{1}{\sinh(\eta)}\left[\mathrm{e}^{-\eta} + \cosh\left(\frac{\alpha-1}{\alpha+1}\eta\right)\right], \tag{70}$$

$$\alpha = \frac{h_1}{h_2}, \quad \delta = \frac{a}{2h}. \tag{71}$$

Once the auxiliary function $\bar{\psi}(\bar{x})$ is determined from Eq. (66), the entire electroelastic field is obtainable. Due to the complicated form of the kernel, it seems unlikely that a closed-form solution can be determined for $\bar{\psi}(\bar{x})$ and therefore one must appeal to either numerical or approximate methods for solving this equation. In effect, by replacing Eq. (66) with a finite system of algebraic equations, a solution to Eq. (66) may be determined by numerical schemes (Baker, 1978).

In particular, the case of small parameter δ is of much interest in practical applications. For this case an approximate solution to Eq. (66) can be constructed by using an iterative approach as follows. For small values of $\delta \ll 1$, we propose a solution to Eq. (66) in the form

$$\bar{\psi}(\bar{x}) = \frac{\tau^{(l)}}{c_{44}} \sum_{n=0}^{\infty} \delta^{2n} \bar{\psi}_{2n}(\bar{x}). \tag{72}$$

Using the expression of $J_0(x)$ in power series form, we find

$$J_0(\bar{u}\eta\delta)J_0(\bar{x}\eta\delta) = 1 - \frac{1}{2^2}(\bar{u}^2 + \bar{x}^2)\eta^2\delta^2 + \frac{1}{2^6}(\bar{u}^4 + 4\bar{u}^2\bar{x}^2 + \bar{x}^4)\eta^4\delta^4 + \mathrm{O}(\delta^6), \tag{73}$$

which permits us to write the kernel (67), $\bar{K}(\bar{x},\bar{u})$, in Eq. (66) in power series form

$$\bar{K}(\bar{x},\bar{u}) = \bar{x} \sum_{n=0}^{\infty} g_{2n}(\bar{x},\bar{u})\delta^{2n+2} \tag{74}$$

with

$$g_0(\bar{x},\bar{u}) = I_0^{(l)}, \quad g_2(\bar{x},\bar{u}) = \frac{1}{2^2} I_1^{(l)}(\bar{x}^2 + \bar{u}^2), \quad g_4(\bar{x},\bar{u}) = \frac{1}{2^6} I_2^{(l)}(\bar{x}^4 + 4\bar{x}^2\bar{u}^2 + \bar{u}^4), \tag{75}$$

where

$$I_n^{(l)} = (-1)^n \int_0^\infty k^{(l)}(\eta)\eta^{2n+1}\,\mathrm{d}\eta. \tag{76}$$

Now substituting $\bar{\psi}(\bar{x})$ and $\bar{K}(\bar{x},\bar{u})$, respectively, from Eqs. (72) and (74) into Eq. (66) and comparing the coefficients of powers of δ from both sides, we obtain an approximate solution, given by Eq. (72), where

$$\bar{\psi}_0(\bar{x}) = \bar{x}, \tag{77}$$

$$\bar{\psi}_{2n}(\bar{x}) = -\bar{x}\sum_{m=1}^{n}\int_0^1 g_{2m-2}(\bar{x},\bar{u})\bar{\psi}_{2n-2m}(\bar{u})\,\mathrm{d}\bar{u}, \quad n = 1,2,3,\ldots \tag{78}$$

By carrying out the iterative process up to $\bar{\psi}_6(\bar{x})$, we get

$$\bar{\psi}_2(\bar{x}) = -\tfrac{1}{2}I_0^{(l)}\bar{x}, \tag{79}$$

$$\bar{\psi}_4(\bar{x}) = -\frac{1}{2^2}\left[I_1^{(l)}\left(\frac{1}{4}+\frac{\bar{x}^2}{2}\right) - \left(I_0^{(l)}\right)^2\right]\bar{x}, \tag{80}$$

$$\bar{\psi}_6(\bar{x}) = -\frac{1}{2^3}\left[I_2^{(l)}\left(\frac{1}{48}+\frac{\bar{x}^2}{8}+\frac{\bar{x}^4}{16}\right) - I_0^{(l)}I_1^{(l)}\left(\frac{1}{4}+\frac{\bar{x}^2}{2}\right) + I_0^{(l)}\left(\left(I_0^{(l)}\right)^2 - \frac{I_1^{(l)}}{2}\right)\right]\bar{x}. \tag{81}$$

Therefore we obtain an approximate solution for small values of δ to be

$$\bar{\psi}(\bar{x}) = \frac{\tau^{(l)}}{c_{44}}\left[\bar{\psi}_0(\bar{x}) + \bar{\psi}_2(\bar{x})\delta^2 + \bar{\psi}_4(\bar{x})\delta^4 + \bar{\psi}_6(\bar{x})\delta^6\right] + \mathrm{O}(\delta^8). \tag{82}$$

In particular, $\bar{\psi}(1)$ can be evaluated approximately by

$$\bar{\psi}(1) = \frac{\tau^{(l)}}{c_{44}}\left[1 - \frac{1}{2}I_0^{(l)}\delta^2 + \frac{1}{2^2}\left(\left(I_0^{(l)}\right)^2 - \frac{3}{4}I_1^{(l)}\right)\delta^4 - \frac{1}{2^3}\left(\left(I_0^{(l)}\right)^3 - \frac{5}{4}I_0^{(l)}I_1^{(l)} + \frac{5}{24}I_2^{(l)}\right)\delta^6 + \mathrm{O}(\delta^8)\right], \tag{83}$$

where the values of $I_n^{(l)}$ may be determined from the asymptotic expressions given in Appendix A.

For many purposes, it is desirable to determine field intensity factors and energy release rate. In particular, in analyzing the stability of a crack in a piezoelectric material, they may be chosen as two important parameters (Pak, 1990; Suo et al., 1992; Gao et al., 1997). Since field intensity factors and energy release rate are closely related to the crack-tip field, it is natural to determine the asymptotic expressions for electroelastic field near the crack tip. This is done in what follows. After neglecting certain lower-order terms, the distribution of $\tau_{zy}(x,0)$ has the following asymptotic expression in the vicinity of the crack tip

$$\tau_{zy1}(x,0^+) = \tau_{zy2}(x,0^-) = c_{44}\bar{\psi}(1)\sqrt{\frac{a}{2r}} + \mathrm{O}(1), \quad r = x-a \ (0 < r/a \ll 1), \tag{84}$$

which further allows us to determine the stress intensity factor at the crack tip

$$K_{\mathrm{III}}^{\tau} = \lim_{x\to a^+}\sqrt{2\pi(x-a)}\,\tau_{zy1}(x,0^+) = c_{44}\bar{\psi}(1)\sqrt{\pi a}. \tag{85}$$

By an analogous treatment, the asymptotic distributions of the components of electric displacement, $D_y(x,0)$, and anti-plane shear strain, $\gamma_{zy}(x,0)$, may be expressed in a unified form in terms of $\bar{\psi}(1)$, i.e.

$$D_y(x,0) = \frac{K_{\mathrm{III}}^{D}}{\sqrt{2\pi r}} + \mathrm{O}(1), \quad \gamma_{zy}(x,0) = \frac{K_{\mathrm{III}}^{\gamma}}{\sqrt{2\pi r}} + \mathrm{O}(1), \tag{86}$$

where

$$K_{\mathrm{III}}^{D} = e_{15}\bar{\psi}(1)\sqrt{\pi a}, \quad K_{\mathrm{III}}^{\gamma} = \bar{\psi}(1)\sqrt{\pi a}. \tag{87}$$

It is easily seen that

$$K_{\mathrm{III}}^{D} = e_{15}K_{\mathrm{III}}^{\gamma}, \quad K_{\mathrm{III}}^{\tau} = c_{44}K_{\mathrm{III}}^{\gamma}. \tag{88}$$

As expected, for all the four cases, the intensity factors of stress, strain, and electric displacement exhibit the square-root singularity at the crack tip, while the tangent component of electric field always vanishes along $y = 0$. Moreover, for cases 1 and 2, the kernel of the governing integral equation (66) is independent of material constants, and it further reveals that in these two cases the stress intensity factor K_{III}^{τ} is independent of material constants, and depends only on the geometric parameters such as the dimensionless crack length a/h and the crack position h_1/h_2. For cases 3 and 4, field intensity factors depends not only on material constants, but also on the geometric parameters.

As a check, in the limiting case as $h_1 \to \infty$, $h_2 \to \infty$ in Eq. (67), we get $\bar{K}^{(l)}(\bar{x}, \bar{u}) = 0$, which then implies the solution of Eq. (66) to be $\bar{\psi}(\bar{x}) = \bar{x}\tau_0/c_{44}$, and furthermore we can derive the corresponding electroelastic field, which is identical to that for a crack in an infinite piezoelectric material by Zhang and Tong (1996).

From the viewpoint of Griffith energy balance, the energy release rate, defined as the change of energy of a cracked medium for an infinitesimal crack extension, is also a significant fracture criterion in piezoelectric materials (Pak, 1990; Suo et al., 1992; Gao et al., 1997). Assume that under applied loadings the crack tip advances along the crack plane from $x = a$ to $a + \delta a$ $(\delta a \ll a)$. Then the energy release rate per unit length during this process is given by

$$G_{\mathrm{III}} = \lim_{\delta a \to 0} \frac{1}{2\,\delta a} \int_0^{\delta a} \left[\tau_{zy}(r, 0)\,\Delta w(\delta a - r, 0) + D_y(r, 0)\,\Delta\phi(\delta a - r, 0)\right] \mathrm{d}r, \tag{89}$$

where r denotes the distance from the crack tip.

It is noted that electric potential is continuous across the crack for a permeable crack, and consequently it has no contribution on energy release rate. As a result, values of the energy release rate coincide with values of the mechanical strain energy release rate proposed by Park and Sun (1995a,b).

To evaluate the energy release rate, it is necessary to determine the crack sliding displacement across the crack surfaces $\Delta w(x, 0)$ $(0 < x < a)$, in particular the asymptotic expression for $\Delta w(x, 0)$ near the crack tip, $x = a - r$ $(0 < r/a \ll 1)$. After some algebra, the final result is

$$\Delta w(x, 0) = w_1(x, 0^+) - w_2(x, 0^-) = 2\bar{\psi}(1)\sqrt{2ar} + \mathrm{O}(r), \quad r = a - x \ (0 < r/a \ll 1). \tag{90}$$

With the asymptotic expressions for $\tau_{zy}(x, 0)$ and $\Delta w(x, 0)$ at hand, the integral given by Eq. (89) can be directly calculated, which is expressed as follows

$$G_{\mathrm{III}} = \frac{\pi a}{2} c_{44}[\bar{\psi}(1)]^2 = \frac{1}{2c_{44}} \left(K_{\mathrm{III}}^{\tau}\right)^2. \tag{91}$$

From the above, we conclude that for a cracked piezoelectric strip of stress-free boundary, energy release rate at the crack tip is independent of electric loadings, while for a cracked piezoelectric strip of clamped boundary, energy release rate at the crack tip depends not only on mechanical loading but also on electric loadings. These conclusions are in accordance with those for a central crack in a piezoelectric strip in Shindo et al. (1997), and those for a crack in an infinite piezoelectric material in Zhang and Tong (1996).

4. Crack situated at the center of a piezoelectric strip

Generally speaking, a closed-form solution is the desired for a majority of problems, and however one usually has to appeal to approximate or numerical approaches for solving some practical problems due to mathematical complications. In this section, a closed-form solution can be obtained for a particular case of a crack situated at the center of a piezoelectric strip, i.e. $h_1 = h_2$. In what follows for convenience cases 1 and 4 will be studied, respectively.

First we consider case 1. In this case, if introducing a new function

$$\varphi(x) = \int_x^a \frac{\psi(u)}{\sqrt{u^2 - x^2}}\,\mathrm{d}u, \tag{92}$$

we find that by virtue of Eq. (41), Eq. (39) is then rewritten as the following form

$$A_1(\xi) = \frac{2}{\pi}\int_0^a \varphi(x)\cos(x\xi)\,\mathrm{d}x, \tag{93}$$

which, in fact, is derived as well in an alternative approach by application of inverted Fourier cosine transform to Eq. (37). In addition, from Eqs. (32) and (37) we observe

$$\varphi(x) = \tfrac{1}{2}[w_1(x, 0^+) - w_2(x, 0^-)] = \tfrac{1}{2}\Delta w(x, 0) \tag{94}$$

and so $\varphi(x) = 0$, $x \geqslant a$.

Substituting Eq. (93) into Eq. (38) yields an integral equation for $\varphi(x)$

$$\frac{2}{\pi}\int_0^a \varphi(u)\,\mathrm{d}u \int_0^\infty \xi\tanh(h\xi)\cos(u\xi)\cos(x\xi)\,\mathrm{d}\xi = \frac{\tau^{(1)}}{c_{44}}, \quad |x| < a. \tag{95}$$

Recalling the known result (Gradshteyn and Ryzhik, 1980)

$$\int_0^\infty \frac{\tanh(h\xi)\cos(t\xi)}{\xi}\,\mathrm{d}\xi = \ln\left|\coth\left(\frac{\pi t}{4h}\right)\right|, \tag{96}$$

we find

$$\int_0^\infty \xi\tanh(h\xi)\cos(u\xi)\cos(x\xi)\,\mathrm{d}\xi = \frac{1}{2}\frac{\mathrm{d}}{\mathrm{d}x}\frac{\mathrm{d}}{\mathrm{d}u}\ln\left|\frac{\sinh(bx) + \sinh(bu)}{\sinh(bx) - \sinh(bu)}\right|, \tag{97}$$

which allows us to rewrite Eq. (95) in the form

$$\frac{1}{\pi}\int_0^a \varphi'(u)\ln\left|\frac{\sinh(bx) + \sinh(bu)}{\sinh(bx) - \sinh(bu)}\right|\mathrm{d}u = \frac{x\tau^{(1)}}{c_{44}}, \quad 0 \leqslant x < a, \tag{98}$$

where $b = \pi/2h$, the integration by parts in deriving the above equation and $\varphi(a) = 0$ have been employed.

Eq. (98) is a singular integral equation with logarithmic kernel. With the aid of the known results (Cooke, 1970; Estrada and Kanwal, 1989), the half of the sliding shear displacement across the crack surfaces is found to be

$$\varphi(x) = -\frac{2\tau^{(1)}}{\pi c_{44}}\int_x^a \frac{F(\pi/2, \tanh(bu))\sinh(bu)}{\sqrt{\sinh^2(bu) - \sinh^2(bx)}}\,\mathrm{d}u, \quad 0 \leqslant x < a \tag{99}$$

and the anti-plane shear stress can also be given explicitly as follows

$$\tau_{zy}(x, 0) = \frac{2\tau^{(1)}}{\pi}\frac{\cosh(ba)\tanh(bx)}{\sqrt{\sinh^2(bx) - \sinh^2(ba)}}\left[F\left(\frac{\pi}{2}, \tanh(ba)\right) - \frac{\sinh^2(bx) - \sinh^2(ba)}{\sinh^2(bx)\cosh^2(ba)} \times \Pi\left(\frac{\pi}{2}, -\frac{\tanh^2(ba)}{\tanh^2(bx)}, \tanh(ba)\right)\right], \quad x > a, \tag{100}$$

where F and Π are the elliptical integrals of the first kind and the third kind, respectively. It is further seen easily from Eqs. (28) and (29) that the normal component of electric displacement is expressed explicitly, which is related to the anti-plane shear stress component by

$$D_y(x,0) = \frac{e_{15}}{c_{44}}\tau_{zy}(x,0), \quad x > a. \tag{101}$$

As expected, the anti-plane shear stress, electric displacement exhibit the usual square-root singularity near the crack tip, and their intensity factors and energy release rate in this case as well can be obtained in explicit form by a straight calculation,

$$K_{\rm III}^{\tau} = \tau^{(1)}\sqrt{\pi a}\frac{2}{\pi}F\left(\frac{\pi}{2},\tanh(ba)\right)\sqrt{\frac{\tanh(ba)}{ba}}, \tag{102}$$

$$K_{\rm III}^{D} = \frac{e_{15}}{c_{44}}\tau^{(1)}\sqrt{\pi a}\frac{2}{\pi}F\left(\frac{\pi}{2},\tanh(ba)\right)\sqrt{\frac{\tanh(ba)}{ba}} \tag{103}$$

and

$$G_{\rm III} = \frac{\left[\tau^{(1)}\right]^2\pi a}{2c_{44}}\left[\frac{2}{\pi}F\left(\frac{\pi}{2},\tanh(ba)\right)\sqrt{\frac{\tanh(ba)}{ba}}\right]^2. \tag{104}$$

If setting $h \to \infty$, i.e. $b \to 0$, the above results revert to those for a permeable crack embedded in an infinite piezoelectric material in Zhang and Tong (1996).

Now we turn our attention to case 4. By an entirely analogous treatment, in view of Eq. (93), Eq. (62) becomes

$$\frac{2}{\pi}\int_0^a \varphi(u)\,\mathrm{d}u\int_0^\infty \xi\coth(h\xi)\cos(u\xi)\cos(x\xi)\,\mathrm{d}\xi = \frac{\tau^{(4)}}{c_{44}}, \quad |x| < a. \tag{105}$$

Recalling the known result (Gradshteyn and Ryzhik, 1980)

$$\int_0^\infty \frac{\coth(h\xi)\cos(t\xi)}{\xi}\,\mathrm{d}\xi = -\ln\left|2\sinh\left(\frac{\pi t}{2h}\right)\right| \tag{106}$$

and proceeding as before, we find

$$\int_0^\infty \xi\coth(h\xi)\cos(u\xi)\cos(x\xi)\,\mathrm{d}\xi = \frac{1}{2}\frac{\mathrm{d}}{\mathrm{d}x}\frac{\mathrm{d}}{\mathrm{d}u}\ln\left|\frac{\tanh(bx)+\tanh(bu)}{\tanh(bx)-\tanh(bu)}\right|, \tag{107}$$

which allows us to rewrite Eq. (105) in the form

$$\frac{1}{\pi}\int_0^a \varphi'(u)\ln\left|\frac{\tanh(bx)+\tanh(bu)}{\tanh(bx)-\tanh(bu)}\right|\mathrm{d}u = \frac{x\tau^{(4)}}{c_{44}}, \quad 0 \leqslant x < a, \tag{108}$$

where $b = \pi/2h$.

Using the known results of a singular integral equation with logarithmic kernel (Cooke, 1970; Estrada and Kanwal, 1989), the solution of Eq. (108), i.e. the half of the sliding shear displacement across the crack surfaces, is found to be

$$\varphi(x) = -\frac{\tau^{(4)}}{bc_{44}}\cos^{-1}\left(\frac{\cosh(bx)}{\cosh(ba)}\right), \quad 0 \leqslant x \leqslant a \tag{109}$$

and the components of anti-plane shear stress and electric displacement are given in explicit form,

$$\tau_{zy}(x,0)=\tau^{(4)}\left[\frac{\sinh(bx)}{\sqrt{\sinh^2(bx)-\sinh^2(ba)}}-1\right],\quad x>a, \tag{110}$$

$$D_y(x,0)=\frac{e_{15}\tau^{(4)}}{c_{44}}\left[\frac{\sinh(bx)}{\sqrt{\sinh^2(bx)-\sinh^2(ba)}}-1\right],\quad x>a. \tag{111}$$

From these expressions for $\tau_{zy}(x,0)$ and $D_y(x,0)$, the anti-plane shear stress and electric displacement also exhibit the usual square-root singularity near the crack tip, and the intensity factors of stress and electric displacement are respectively

$$K_{\mathrm{III}}^{\tau}=\tau^{(4)}\sqrt{\pi a}\sqrt{\frac{2h}{\pi a}\tanh\left(\frac{\pi a}{2h}\right)}, \tag{112}$$

$$K_{\mathrm{III}}^{D}=\frac{e_{15}}{c_{44}}\tau^{(4)}\sqrt{\pi a}\sqrt{\frac{2h}{\pi a}\tanh\left(\frac{\pi a}{2h}\right)}. \tag{113}$$

The energy release rate in this case is

$$G_{\mathrm{III}}=\frac{\left[\tau^{(4)}\right]^2h}{c_{44}}\tanh\left(\frac{\pi a}{2h}\right), \tag{114}$$

which indicates that in view of Eq. (18) both the mechanical loading and electric loading have influence on the energy release rate for the case of clamped boundaries. The energy release rate for a permeable crack is always positive, irrespective of positive or negative electric field, and the magnitude, however, varies with the direction of electric field. In other words, the change of direction of electric field will enhance or retard the propagation of a crack.

The results obtained by Zhang and Tong (1996) are recovered again from a limiting case, $h\to\infty$, of the present results. On the other hand, for another limiting case, i.e. a semi-infinite crack lying in the center of a piezoelectric strip, the electroelastic field can be straightforwardly obtained by a limiting procedure from the above results. That is, replacing x with $a+x_1$ in the electroelastic field given above, and then setting $a\to\infty$, we find that analytical expressions for the desired anti-plane shear stress and electric displacement are respectively

$$\tau_{zy}(x_1,0)=\tau^{(4)}\left[\frac{\mathrm{e}^{bx_1/2}}{\sqrt{2\sinh(bx_1)}}-1\right],\quad x_1>0, \tag{115}$$

$$D_y(x_1,0)=\frac{e_{15}\tau^{(4)}}{c_{44}}\left[\frac{\mathrm{e}^{bx_1/2}}{\sqrt{2\sinh(bx_1)}}-1\right],\quad x_1>0, \tag{116}$$

which allow us to evaluate the intensity factors of stress and electric displacement near the crack tip as

$$K_{\mathrm{III}}^{\tau}=\tau^{(4)}\sqrt{2h},\quad K_{\mathrm{III}}^{D}=\frac{e_{15}\tau^{(4)}}{c_{44}}\sqrt{2h} \tag{117}$$

and the energy release rate as

$$G_{\mathrm{III}}=\frac{\left[\tau^{(4)}\right]^2h}{c_{44}}. \tag{118}$$

5. Results and discussion

Numerical results for the normalized energy release rate G_{III}/G_∞, G_∞ being the energy release rate as $h_1 \to \infty$ and $h_2 \to \infty$, are presented. It is noted that in the expression for G_∞ for cases 3 and 4, w_0/h and V_0/h are understood as constants γ_0 and E_0, respectively, as $h \to \infty$. Taking into account

$$G_{III}/G_\infty = \left[\frac{c_{44}}{\tau^{(l)}}\bar{\psi}(1)\right]^2 = \left[\bar{\psi}_0(1) + \delta^2\bar{\psi}_2(1) + \cdots + \delta^{2n}\bar{\psi}_{2n}(1) + \mathrm{O}(\delta^{2n+2})\right]^2, \tag{119}$$

where $\bar{\psi}_0(1), \bar{\psi}_2(1), \ldots$, are given by Eqs. (77) and (79), etc., it is easily seen that G_{III}/G_∞ is independent of material constants except for case 3.

Theoretically, the higher the order of δ in the terms appearing in the above expression is, the more accurate approximate value of G_{III}/G_∞ is. However, for a given order of δ, experience shows that it is the best to take

$$G_{III}/G_\infty = \left[\bar{\psi}_0(1) + \delta^2\bar{\psi}_2(1) + \cdots + \tfrac{1}{2}\delta^{2n}\bar{\psi}_{2n}(1)\right]^2 \tag{120}$$

instead of

$$G_{III}/G_\infty = \left[\bar{\psi}_0(1) + \delta^2\bar{\psi}_2(1) + \cdots + \delta^{2n}\bar{\psi}_{2n}(1)\right]^2. \tag{121}$$

This is demonstrated in Figs. 2 and 3 for cases 1 and 4, respectively, in which the solid line is generated from the analytical expressions

$$G_{III}/G_\infty = \left[\frac{2}{\pi}F\left(\frac{\pi}{2}, \tanh\left(\frac{\pi a}{2h}\right)\right)\right]^2 \frac{2h}{\pi a}\tanh\left(\frac{\pi a}{2h}\right) \tag{122}$$

for case 1 and

$$G_{III}/G_\infty = \frac{2h}{\pi a}\tanh\left(\frac{\pi a}{2h}\right) \tag{123}$$

for case 4, and the other lines are generated from some approximate expressions (120) and (121) for $n = 3$ and 2.

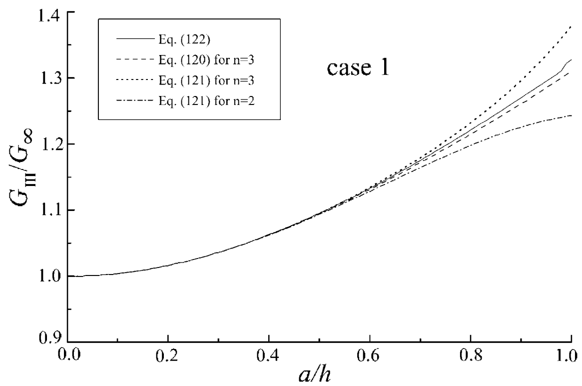

Fig. 2. Comparison of exact value and approximate value of the normalized energy release rate for case 1.

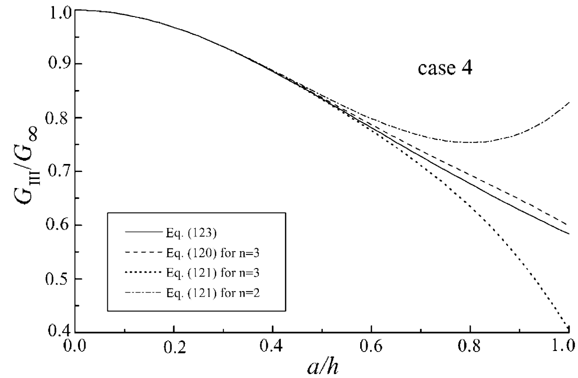

Fig. 3. Comparison of exact value and approximate value of the normalized energy release rate for case 4.

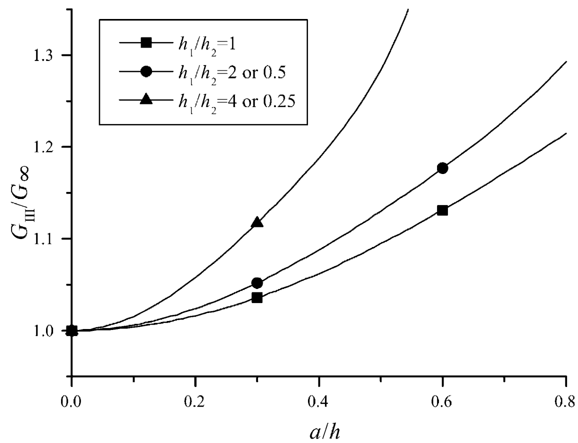

Fig. 4. Variation of the normalized energy release rate G_{III}/G_∞ versus the dimensionless crack length a/h for several different crack positions $h_1/h_2 = 0.25$, 0.5, 1, 2, 4 for case 1.

Evaluating G_{III}/G_∞ by using Eq. (120), Figs. 4–6 show that the variation of the normalized energy release rate G_{III}/G_∞ versus the normalized crack length a/h when the ratio $h_1/h_2 = 0.25$, 0.5, 1, 2, 4, for cases 1, 3, and 4, respectively. It is observed that with increasing a/h, G_{III}/G_∞ increases for a piezoelectric strip of stress-free boundary, and decreases for a strip of clamped boundary. In Figs. 7–9, the variation of G_{III}/G_∞ versus the crack position, denoted as h_1/h_2, is plotted with $a/h = 0.01$, 0.1, 0.3 for cases 1, 3, and 4, respectively. From these figures it is found that when a crack is located at the center of a piezoelectric strip, G_{III}/G_∞ arrives at the minimum for the case of stress-free boundary and the maximum for the case of clamped boundary. As a result, we conclude that a central crack in a piezoelectric strip of stress-free boundary is more easy to extend than an eccentric crack, while an eccentric crack in a piezoelectric strip of clamped boundary is more easy to extend than a central crack.

For case 3, the variation of G_{III}/G_∞ versus the electromechanical coupling factor $e_{15}/(c_{44}\varepsilon_{11})^{1/2}$ is presented graphically for different crack position h_1/h_2 and dimensionless crack length a/h, which reveals that the electromechanical coupling factor has an apparent influence on the normalized energy release rate G_{III}/G_∞. In principle, G_{III}/G_∞ decreases as $e_{15}/(c_{44}\varepsilon_{11})^{1/2}$ increases (Fig. 10).

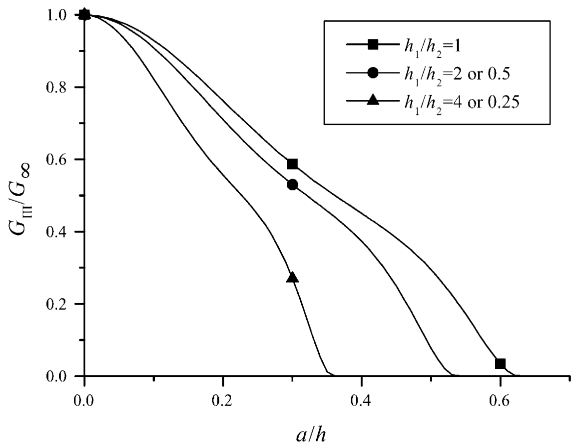

Fig. 5. Variation of the normalized energy release rate G_{III}/G_∞ versus the dimensionless crack length a/h for several different crack positions $h_1/h_2 = 0.25$, 0.5, 1, 2, 4 for case 3.

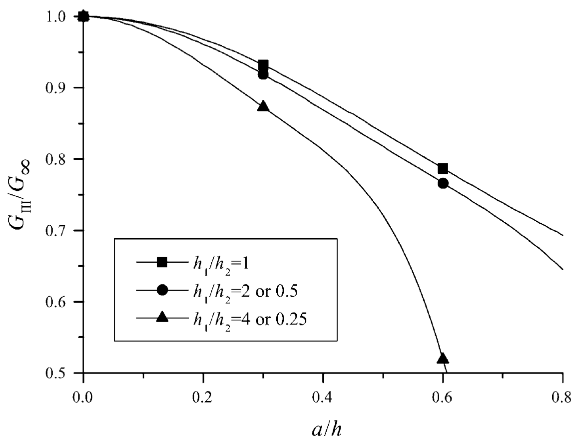

Fig. 6. Variation of the normalized energy release rate G_{III}/G_∞ versus the dimensionless crack length a/h for several different crack positions $h_1/h_2 = 0.25$, 0.5, 1, 2, 4 for case 4.

6. Conclusions

The problem involving a piezoelectric strips with a through anti-plane shear crack is analyzed under the action of four cases of combined electromechanical loadings. Using an integral transform technique, dual integral equations resulting from the mixed boundary value problem are further converted into a Fredholm integral equation for a new auxiliary function, which is solved analytically by an approximate method. The intensity factor of electroelastic field and the energy release rate are explicitly expressed in terms of the introduced auxiliary function. For a crack lying at the center of a piezoelectric strip, closed-form solutions for cases 1 and 4 are obtained, respectively. The results indicate that the energy release rate is independent of electric loadings for a piezoelectric strip of stress-free boundary and depends on both electric loadings and mechanical loadings for a piezoelectric strip of clamped boundary. Numerical results are presented graphically to show the dependance of field intensity factors and energy release rate on material constants and geometric parameters.

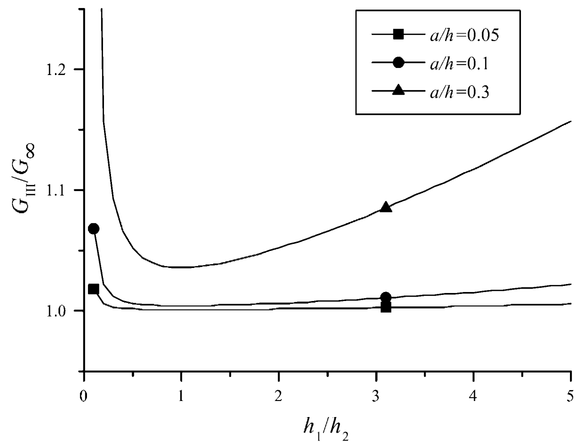

Fig. 7. Variation of the normalized energy release rate G_{III}/G_{∞} versus the crack position h_1/h_2 for dimensionless crack length $a/h = 0.05, 0.1, 0.3$ for case 1.

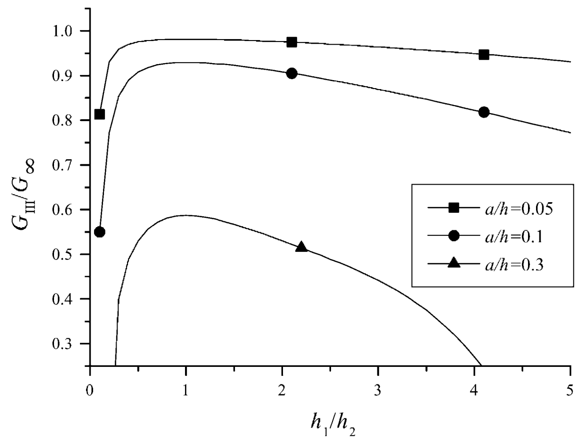

Fig. 8. Variation of the normalized energy release rate G_{III}/G_{∞} versus the crack position h_1/h_2 for dimensionless crack length $a/h = 0.05, 0.1, 0.3$ for case 3.

Acknowledgements

This work was supported by Major State Basic Research Project of the Ministry of Science and Technology of China.

Appendix A

Using the following asymptotic relation

$$\frac{\eta}{\sinh(\eta)} = (1 + 0.76734\eta)e^{-2.7316\eta} + 2\eta e^{-\eta},$$

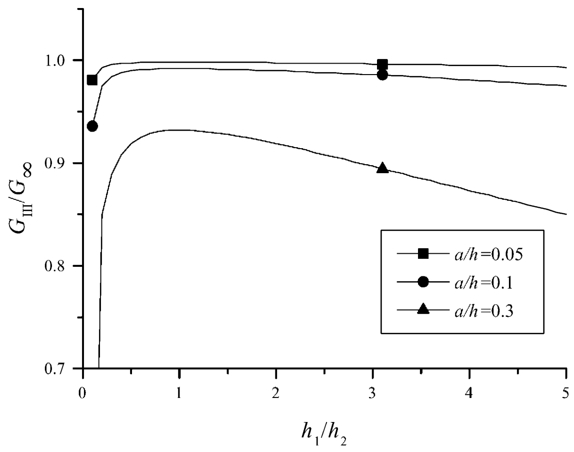

Fig. 9. Variation of the normalized energy release rate G_{III}/G_∞ versus the crack position h_1/h_2 for dimensionless crack length $a/h = 0.05$, 0.1, 0.3 for case 4.

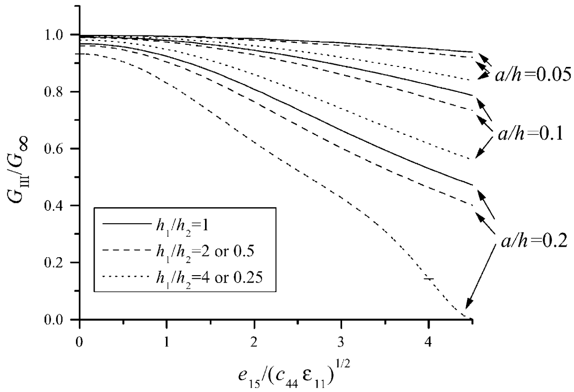

Fig. 10. Variation of the normalized energy release rate G_{III}/G_∞ versus the electromechanical coupling factor $e_{15}/(c_{44}\varepsilon_{11})^{1/2}$ for different crack position h_1/h_2 and dimensionless crack length a/h for case 3.

which is established by Keer and Lin (1987), who treated the crack problem of in an elastic layer of fixed surfaces, one can obtain a simple, approximate, analytical formula for evaluating $I_n^{(l)}$, which can evaluated by separating into two parts M_n and N_n,

$$M_n = \int_0^\infty \frac{\eta^{2n+1}}{\sinh(\eta)} \mathrm{e}^{-\eta}\, \mathrm{d}\eta,$$
$$N_n = \int_0^\infty \frac{\eta^{2n+1}}{\sinh(\eta)} \cosh\left(\frac{\alpha - 1}{\alpha + 1}\eta\right) \mathrm{d}\eta,$$

where M_n and N_n have the following asymptotic expressions:

$$M_n = \frac{(2n)!}{2}\left[\frac{2(1.206 + 0.411n)}{3.7316^{2n+1}} + \frac{2n+1}{4^n}\right]$$

$$N_n = \frac{(2n)!}{2}\left\{\left[\left(\frac{1+\alpha}{1.7316+3.7316\alpha}\right)^{2n+1} + \left(\frac{1+\alpha}{3.7316+1.7316\alpha}\right)^{2n+1}\right]\right.$$
$$+ 0.76734(2n+1)\left[\left(\frac{1+\alpha}{1.7316+3.7316\alpha}\right)^{2n+2} + \left(\frac{1+\alpha}{3.7316+1.7316\alpha}\right)^{2n+2}\right]$$
$$\left. + 2(2n+1)\left[\left(\frac{1+\alpha}{2\alpha}\right)^{2n+2} + \left(\frac{1+\alpha}{2}\right)^{2n+2}\right]\right\}.$$

References

Baker, C.T.H., 1978. The Numerical Treatment of Integral Equations. Clarendon Press, Oxford.

Chen, W.Q., Shioya, T., 1999. Fundamental solution for a penny-shaped crack in a piezoelectric medium. J. Mech. Phys. Solids 47, 1459–1475.

Cooke, J.C., 1970. The solution of some integral equations and their connection with dual integral equation and series. Glasgow Math. J. 11, 9–20.

Dascalu, C., 1997. Electroelasticity equations and energy approaches to fracture. Int. J. Engng. Sci. 35, 1185–1194.

Dascalu, C., Maugin, G.A., 1995. On the dynamic fracture of piezoelectric materials. Quart. J. Mech. Appl. Math. 48, 237–255.

Dunn, M.L., 1994. The effects of crack face boundary conditions on the fracture mechanics of piezoelectric solids. Engng. Fract. Mech. 48, 25–39.

Estrada, P., Kanwal, R.P., 1989. Integral equations with logarithmic kernels. IMA J. Appl. Math. 45, 133–155.

Gao, H., Zhang, T.-Y., Tong, P., 1997. Local and global the energy release rates for an electrically yielded crack in a piezoelectric ceramics. J. Mech. Phys. Solids 45, 491–510.

Gradshteyn, I.S., Ryzhik, I.M., 1980. Table of Integrals, Series and Products. New York, Academic Press.

Keer, L.M., Lin, W., 1987. A penny-shaped crack in a layer whose upper and lower surfaces are fixed. Int. J. Fract. 34, 229–236.

Kwon, S.M., Lee, K.Y., 2000. Analysis of stress and electric fields in a rectangular piezoelectric body with a center crack under anti-plane shear loading. Int. J. Solids Struct. 37, 4859–4869.

Meguid, S.A., Wang, X.D., 1998. Dynamic anti-plane behavior of interacting cracks in a piezoelectric medium. Int. J. Fract. 91, 391–403.

Narita, F., Shindo, Y., 1999. The interface crack problem for bonded piezoelectric and orthotropic layers under antiplane shear loading. Int. J. Fract. 98, 87–101.

Pak, Y.E., 1990. Crack extension force in a piezoelectric material. J. Appl. Mech. 57, 863–869.

Pak, Y.E., 1992. Linear electro-elastic fracture mechanics of piezoelectric materials. Int. J. Fract. 54, 79–100.

Park, S., Sun, C.-T., 1995a. Effect of electric field on fracture of piezoelectric ceramics. Int. J. Fract. 70, 203–216.

Park, S., Sun, C.-T., 1995b. Fracture criteria for piezoelectric ceramics. J. Am. Ceram. Soc. 78, 1475–1480.

Parton, V.Z., 1976. Fracture mechanics of piezoelectric materials. Acta Astronautica, 3, 671–683.

Parton, V.Z., Kudryavsev, B.A., 1988. Electromagnetoelasticity. Gordon and Breach, New York.

Shin, J.W., Kwon, S.M., Lee, K.Y., 2000. Eccentric crack in a piezoelectric strip under electromechanical loading. J. Appl. Mech. 67, 846–847.

Shindo, Y., Ozawa, E., Nowacki, J.P., 1990. Singular stress and electric fields of a cracked piezoelectric strip. Int. J. Appl. Electromag. Mater. 1, 77–88.

Shindo, Y., Narita, F., Tanaka, K., 1996. Electroelastic intensification near anti-plane shear crack in orthotropic piezoelectric ceramic strip. Theor. Appl. Fract. Mech. 25, 65–71.

Shindo, Y., Tanaka, K., Narita, F., 1997. Singular stress and electric fields of a piezoelectric ceramic layer with a finite crack under longitudinal shear. Acta Mech. 120, 31–45.

Shindo, Y., Watanabe, K., Narita, F., 2000. Electroelastic analysis of a piezoelectric ceramic strip with a central crack. Int. J. Engng. Sci. 38, 1–19.

Sneddon, I.N., 1972. The Use of Integral Transforms. McGraw-Hill, New York.

Sosa, H., 1991. Plane problems in piezoelectric media with defects. Int. J. Solids Struct. 28, 491–505.

Sosa, H., 1992. On the fracture mechanics of piezoelectric solids. Int. J. Solids Struct. 29, 2622–2643.

Sosa, H., Khutoryansky, N.M., 1996. New developments concerning piezoelectric materials with defects. Int. J. Solids Struct. 33, 3399–3414.

Suo, Z., Kuo, C.-M., Barnett, D.M., Willis, J.R., 1992. Fracture mechanics for piezoelectric ceramics. J. Mech. Phys. Solids 40, 739–765.

Wang, B., 1992. Three-dimensional analysis of a flat elliptical crack in a piezoelectric material. Int. J. Engng. Sci. 30, 781–791.

Wang, X.D., 2001. The dynamic behaviour of interacting interfacial cracks in piezoelectric media. Int. J. Solids Struct. 38, 815–831.

Wang, T.C., Han, X.L., 1999. Fracture mechanics of piezoelectric materials. Int. J. Fract. 98, 15–35.

Wang, B.L., Han, J.C., Du, S.Y., 2000. New considerations for the fracture of piezoelectric materials under electromechanical loading. Mech. Res. Commun. 27, 435–444.

Yang, F., 2001. Fracture mechanics for a mode I crack in piezoelectric materials. Int. J. Solids Struct. 38, 3813–3830.

Zhang, P.-Y., Tong, P., 1996. Fracture mechanics for a mode III crack in a piezoelectric material. Int. J. Solids Struct. 33, 343–359.

Zhang, P.-Y., Qian, C.F., Tong, P., 1998. Linear electro-elastic analysis of a cavity or a crack in a piezoelectric material. Int. J. Solids Struct. 35, 2121–2149.

Zhong, S.M., Meguid, S.A., 1997. Analysis of a circular arc-crack in piezoelectric materials. Int. J. Fract. 84, 143–158.